Biophysical Chemistry, 33 (1989) 153–160
Elsevier

BPC 01351

Kinetic study on the dimer-tetramer interconversion of phosphorylase *b* by a stopped-flow X-ray scattering method

Zhi-Xin Wang [a,*], Hirotsugu Tsuruta [b], Yoko Honda [c], Yoshiaki Tachi-iri [d,**], Katsuzo Wakabayashi [e], Yoshiyuki Amemiya [f] and Hiroshi Kihara [a]

[a] *Jichi Medical School, School of Nursing, Minamikawachi, Tochigi 329-04,* [b] *Department of Materials Science, Faculty of Science, Hiroshima University, Higashisenda, Hiroshima 730,* [c] *Department of Agricultural Chemistry, Faculty of Agriculture, Utsunomiya University, Utsunomiya 320,* [d] *Department of Chemistry, Faculty of Science, Science University of Tokyo, Kagurazaka, Shinjuku, Tokyo 162,* [e] *Department of Biophysical Engineering, Faculty of Engineering Science, Osaka University, Toyonaka, Osaka 560 and* [f] *Photon Factory, National Laboratory for High Energy Physics, Oho, Tsukuba, Ibaraki 305, Japan*

Received 11 October 1988
Revised manuscript received 13 January 1989
Accepted 17 January 1989

Stopped-flow; X-ray scattering; Phosphorylase *b*; Kinetics

The dimer-tetramer interconversion of phosphorylase *b* induced by the binding of AMP and Mg^{2+} was monitored using a stopped-flow X-ray scattering method. The rate constants of this second-order reaction have been determined by a nonlinear least-squares method. Burst phases in both radii of gyration and zero-angle intensities were detected at the initial step of the reaction. This suggests that rapid association might take place, followed by a slow association process of which the kinetics were measured in the present study. The radius of gyration of tetrameric phosphorylase *b* was determined and found to be in excellent agreement with that of phosphorylase *a*, but different from that of phosphorylase *b* reported elsewhere (G. Puchwein, O. Kratky, C.F. Golker and E. Helmreich, Biochemistry 9 (1970) 4691). The reason for this inconsistency is discussed.

1. Introduction

Phosphorylase, an enzyme catalyzing glycogen degradation, plays an important role in the regulation of glycogen metabolism in muscle. It exists in two interconvertible forms: phosphorylase *b* and *a*. In conversion of phosphorylase *b* to *a*, a seryl OH side chain of the phosphorylase protomer *b* is phosphorylated through the action of phosphorylase *b* kinase, together with ATP and Mg^{2+}. The reverse reaction, conversion of phosphorylase *a* to *b*, is catalyzed by phosphorylase phosphatase. Phosphorylase *a* and *b* are composed of four or two identical subunits of molecular weight 96 000 under physiological conditions, respectively. It has been observed that the interconversion equilibrium between the dimeric and tetrameric forms of phosphorylase *b* is completely shifted toward the dissociated form in the absence of effectors at any temperature [1].

Two AMP-binding sites have been detected on each enzymatic subunit via different techniques [2,3]. AMP binding might exert a significant effect on both activity and association of the enzyme. The presence of certain divalent cations, such as Mg^{2+}, Ca^{2+} and Mn^{2+}, increases the affinity of the enzyme for AMP, which implies a rise in the extent of tetramerization [5].

Correspondence address: H. Kihara, Jichi Medical School, School of Nursing, Minamikiwachi, Tochigi 329-04, Japan.

* On leave from the Laboratory of Molecular Enzymology, Institute of Biophysics, Academia Sinica, Beijing 100080, P.R. China.

** Present address: Hamamatsu Photonics, Ichino-cho, Hamamatsu 435, Japan.

X-ray scattering provides a useful tool for studying the conformation of macromolecules in solution. Direct information is thereby available on the gross conformation of biological macromolecules [5–8]. Since synchrotron radiation has been used as an intense X-ray source, the time-resolved study of X-ray scattering has been considered most promising. This procedure has been applied in studies on the dissociation of aspartate transcarbamylase [9,10], assembly of hemoglobin subunits [11] and assembly of bromomosaic virus [13]. In this paper, we report the kinetics of the dimer-tetramer interconversion of phosphorylase *b* monitored by using a stopped-flow X-ray scattering method and the influence of Mg^{2+} concentration on the kinetic parameters.

2. Materials and methods

Phosphorylase *b* was purified from rabbit skeletal muscle according to the method of Fischer and Krebs [13]. On average, 500 mg phosphorylase *b* was extracted from 500 g skeletal muscle. Enzyme concentration was determined spectrophotometrically using an extinction coefficient of $E^{1\%}_{1\,cm} = 13.2$ at 280 nm [14].

Enzymatic activity of phosphorylase *b* was estimated by measuring the phosphate produced from glycogen and glucose 1-phosphate; the reverse process of the native reaction in vivo. The phosphate produced was quantitated as described by Fiske and Subbarow with some modifications [15,16]. Enzyme activity was estimated from the slope of a straight line through the origin of a plot of phosphate produced vs. time.

X-ray scattering experiments were performed with a stopped-flow apparatus at beam line 15A1 of the Photon Factory, National Laboratory for High Energy Physics. The camera and detection systems have been reported in detail elsewhere [17,18]. In this experiment, the sample solution was irradiated with monochromatic X-rays (1.55 Å) and scattered X-ray intensities were recorded on a position-sensitive proportional counter (512 channels) of camera length 2403 mm and channel width 0.368 mm. For all X-ray scattering measurements, scattered X-ray intensities were corrected in order to cancel out the effect of the intensity decay of the incident X-ray beam by means of the ionization current of an ion chamber placed in front of the sample cell. The scattering data were normalized with respect to exposure time and enzyme concentration. Normalized data were also subjected to background subtraction. In the present study, X-ray scattering data are expressed in terms of $h = 4\pi \sin\theta/\lambda$, and have been analysed in the form of Guinier plots.

50 mM β-glycerophosphate/mercaptoethanol (pH 6.8) was used as a pH buffer solution in all experiments. The temperature of solutions was maintained at $25 \pm 0.1°C$ throughout. All reagents used were of guaranteed or better grade.

3. Theoretical basis for data analysis

X-ray scattering investigation affords us the structural parameters of the macromolecule. In particular, the radius of gyration and zero-angle intensity, which is proportional to the number of electrons in the molecule, are obtained directly from Guinier plots of the X-ray scattering data. Our intention is the elucidation of the dimer-tetramer interconversion in terms of these two parameters.

The dimer-tetramer interconversion of phosphorylase *b* is represented by:

$$2D^* \underset{k_b}{\overset{k_a}{\rightleftharpoons}} T^*$$

where D* and T* designate the dimer and tetramer, respectively. k_a and k_b are the rate constants of the association and dissociation process, respectively.

The molar fraction of tetramer in the unit of dimer concentration, W, and the dimer fraction, $1 - W$, are defined as:

$$W = \frac{2[T^*]}{[E]}$$

$$1 - W = \frac{[D^*]}{[E]} \qquad (1)$$

where [D*] and [T*] denote total concentration

of dimer and tetramer, respectively. [E] represents the total concentration of enzyme in the unit of dimer concentration, i.e., $[E] = [D^*] + 2[T^*]$.

The zero-angle scattering intensity $I(0)$ of the binary system is given by,

$$I(0) = 0.5WI_T(0) + (1 - W)I_D(0) \quad (2)$$

where $I_T(0)$ and $I_D(0)$ are the zero-angle intensities of tetramer and dimer, respectively. Using the relationship $I_T(0) = 4I_D(0)$, this equation can be written as:

$$I(0) = 2WI_D(0) + (1 - W)I_D(0)$$
$$= (1 + W)I_D(0).$$

Therefore, we obtain the tetramer fraction, W, in terms of zero-angle scattering intensities:

$$W = [I(0)/I_D(0)] - 1. \quad (3)$$

Assuming that phosphorylase b is in the dimeric form in the absence of both AMP and Mg^{2+}, we can obtain the value $I_D(0)$. Thus, the tetramer fraction W can be evaluated using eq. 3. In the present study, the tetramer fraction W did not reach unity even at high Mg^{2+} concentrations as shown in table 1. As a consequence, the radius of gyration of the tetramer could not be obtained directly.

The apparent radius of gyration, R_g, of the binary system is related to the radii of gyration of tetramer and dimer as:

$$R_g^2 = \frac{0.5MW_T^2R_T^2 + (1 - W)M_D^2R_D^2}{0.5WM_T^2 + (1 - W)M_D^2} \quad (4)$$

Table 1

Tetramer fractions and ratios α (R_T/R_D) in equilibrium at different Mg^{2+} concentrations in the presence of 1 mM AMP

$[Mg^{2+}]$ (mM)	W	α
0	0.22	1.26
10	0.63	1.21
25	0.77	1.21
50	0.83	1.24
100	0.83	1.24

where M_T and R_T denote the molecular weight and radius of gyration of the tetramer, respectively, with M_D and R_D corresponding to those of the dimer. Using the relationship $M_T = 2M_D$, the apparent radius of gyration can be reduced to give:

$$R_g^2 = \frac{2WR_T^2 + (1 - W)R_D^2}{1 + W} \quad (5)$$

or

$$\alpha^2 = \frac{R_T^2}{R_D^2} = \frac{\left[R_g^2(1 + W)/R_D^2\right] - 1 + W}{2W}. \quad (6)$$

Since R_D is determined from the scattering curve in the absence of both AMP and Mg^{2+}, as in the case for $I_D(0)$, we can calculate the value α for any tetramer fraction W. As listed in table 1, α is nearly constant at any Mg^{2+} concentration, which implies the validity of this approach. We can then estimate the radius of gyration of tetramer R_T using eq. 6.

In the stopped-flow study, tetramerization of phosphorylase b was initiated by mixing with AMP and Mg^{2+}. The rate equation for this process can be expressed as:

$$\frac{d[T^*]}{dt} = k_a[D^*]^2 - k_b[T^*]$$
$$= k_a([E] - 2[T^*])^2 - k_b[T^*]$$
$$= k_a[E]^2 - (4k_a[E] + k_b)[T^*]$$
$$+ 4k_a[T^*]^2. \quad (7)$$

On equilibrium being attained, $d[T^*]/dt = 0$, i.e.,

$$\frac{d[T^*]}{dt} = k_a([E] - 2[T^*]_{eq})^2 - k_b[T^*]_{eq} = 0$$

then

$$\frac{k_b}{k_a} = \frac{([E] - 2[T^*]_{eq})^2}{[T^*]_{eq}} = \frac{2[E](1 - W_{eq})^2}{W_{eq}}$$
$$= \frac{2[E](1 + W_{eq}^2)}{W_{eq}} - 4[E] \quad (8)$$

where subscript eq designates the equilibrium value. Introducing eqs. 1 and 8 into eq. 7, we obtain:

$$\frac{dW}{dt} = 2[E]k_a\left[1 - \frac{(1+W_{eq}^2)W}{W_{eq}} + W^2\right]$$

$$= 2[E]k_a(W - W_{eq}^{-1})(W - W_{eq}). \quad (9)$$

Integration of this equation under the boundary condition, $W = W_0$ at $t = 0$, yields the following solution for the differential equation:

$$\ln\frac{1 - W_{eq}W}{1 - W_{eq}^{-1}W} = \ln\frac{1 - W_{eq}W_0}{1 - W_{eq}^{-1}W} + \frac{2[E](1 - W_{eq}^2)}{W_{eq}}k_a t$$

$$= -\ln A + Ct. \quad (10)$$

Since W_{eq} can be obtained from eq. 3, a plot of $\ln[(1 - W_{eq}W)/(1 - W_{eq}^{-1}W)]$ vs. time t should give a straight line. We can calculate k_a from the slope of the straight line and obtain k_b further from eq. 8.

Eq. 10 can also be written as:

$$W = \frac{1 - Ae^{-ct}}{W_{eq}^{-1} - W_{eq}Ae^{-ct}}. \quad (11)$$

Introducing eq. 11 into eqs. 3 and 5, the zero-angle scattering intensity and apparent radius of gyration at time t after mixing can then be obtained:

$$I(0) = I_D(0)\left(1 + \frac{1 - Ae^{-ct}}{W_{eq}^{-1} - W_{eq}Ae^{-ct}}\right) \quad (12)$$

$$R_g^2 = R_D^2\left[1 + \frac{2(\alpha^2 - 1)(1 - Ae^{-ct})}{(1 + W_{eq}^{-1}) - (1 + W_{eq})Ae^{-ct}}\right] \quad (13)$$

According to eqs. 12 and 13, the rate constants k_a and k_b can also be obtained by fitting the experimental time course with a nonlinear least squares method.

4. Results

4.1. Solution X-ray scattering in equilibrium

Solution X-ray scattering patterns of phosphorylase b were recorded in the absence or presence of 1 mM AMP and various concentrations of magnesium acetate. The intensities were normalized with respect to concentration and exposure time, and the background scattering patterns for each data set were subtracted.

Fig. 1 shows Guinier plots of a small-angle region. Unbroken lines represent the least-squares fits [19]. One can observe that the radius of gyration R_g and zero-angle intensity $I(0)$ increase upon binding of AMP and Mg^{2+}. In the absence of AMP and Mg^{2+}, R_g was estimated as 39.32 Å ($0.018 < h < 0.028$ Å^{-1}), in excellent agreement with the value reported in ref. 20. It may also be noted that the linear regions can be expanded to the greater value of h ($h < 0.028$ Å^{-1}). In the presence of 1 mM AMP and 100 mM Mg^{2+}, the tetramer fraction W was 0.83 by substituting $I(0)/I_D(0) = 1.83$ into eq. 3. This result at least implies that most of the dimeric phosphorylase b associates into the tetrameric form upon ligation

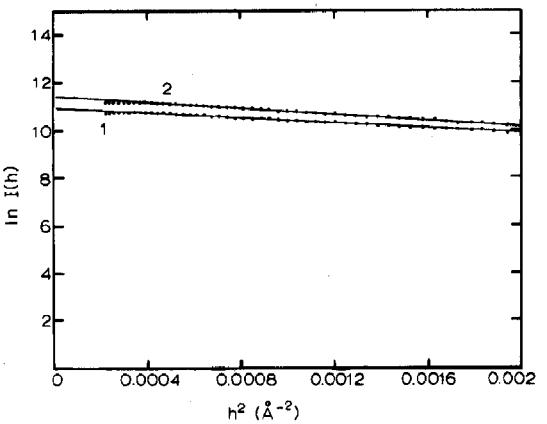

Fig. 1. Guinier plots of solution X-ray scattering data for phosphorylase b in the absence (trace 1) and presence (trace 2) of 1 mM AMP and 100 mM Mg^{2+}; enzyme concentration, 12 mg/ml. Scattering intensities are normalized for incident beam intensity, exposure time and enzyme concentration. Background scattering intensities have been subtracted. Solution contained 50 mM β-glycerophosphate mercaptoethanol as pH buffer (pH 6.8); 25 °C.

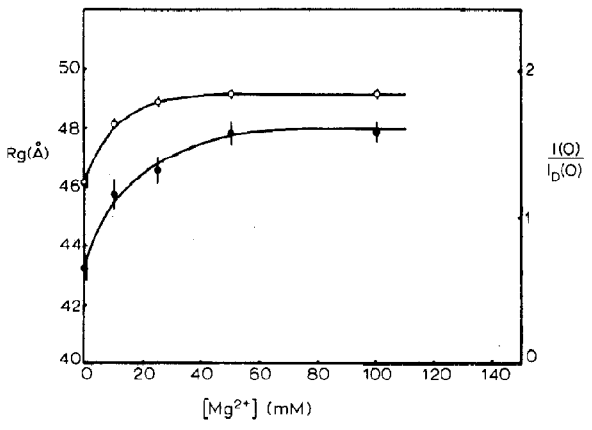

Fig. 2. Effects of Mg^{2+} concentration on R_g (●) (scale on left ordinate) and $I(0)/I_D(0)$ (○) (scale on right ordinate). Other conditions as in fig. 1.

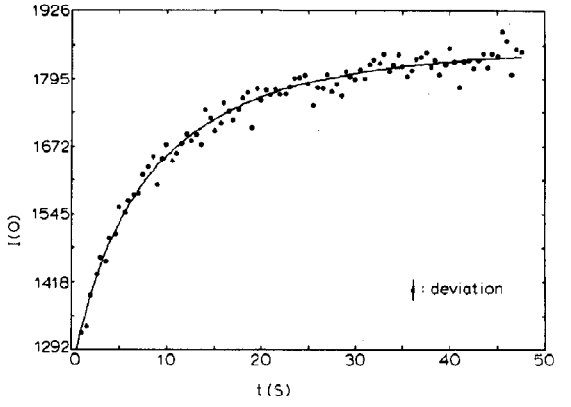

Fig. 4. Time course of zero-angle intensity $I(0)$ for tetramerization of phosphorylase b. Final concentrations: 1 mM AMP and 100 mM Mg^{2+}. Data of 15 shots were accumulated. (———) Theoretical time course calculated from eq. 12 with $I(0) = 1015$, $W_{eq} = 0.83$, $A = 0.89$, $C = 0.029$. Other conditions as in fig. 3.

with AMP and Mg^{2+}. Fig. 2 demonstrates the effects of Mg^{2+} concentration on R_g and $I(0)/I_D(0)$ in the presence of 1 mM AMP. Both parameters increase with increase in Mg^{2+} concentration. R_g increases from 43.2 to 48 Å asymptotically with rise in Mg^{2+} concentration. The values of W_{eq} and α ($= R_T/R_D$) under different conditions are listed in table 1. Using an average value of $\alpha = 1.232$, the radius of gyration of the AMP-ligated tetramer R_T is calculated to be $39.32 \times 1.232 = 48.4 \pm 0.6$ Å, which is consistent with the value for tetrameric phosphorylase a determined previously [23].

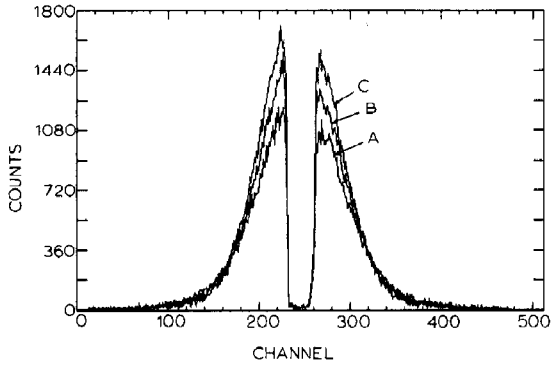

Fig. 3. Time-resolved X-ray scattering patterns of phosphorylase b at different times after mixing with AMP and Mg^{2+}. Final concentrations: 1 mM AMP and 100 mM Mg^{2+}. Respective patterns A–C were recorded at 0.5, 5 and 47 s after mixing. Other conditions as in fig. 1.

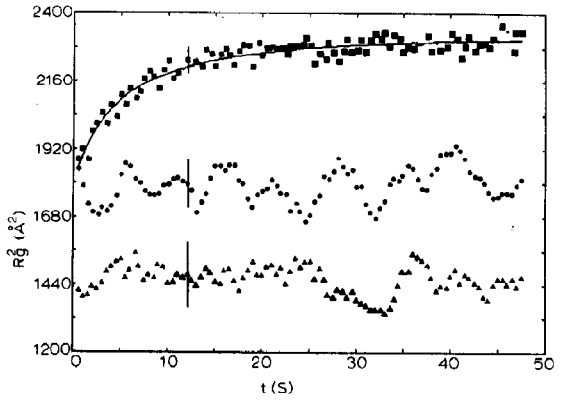

Fig. 5. Time course of variation in radius of gyration R_g with tetramerization of phosphorylase b. Final concentrations: (■) 1 mM AMP and 100 mM Mg^{2+} (15 shots accumulated); (●) 1 mM AMP without Mg^{2+} (4 shots accumulated); (▲) without AMP and Mg^{2+} (2 shots accumulated). Data were smoothed by the method of moving averages (7 points). (———) Theoretical time course calculated from eq. 13 with $R_D = 1565$, $W_{eq} = 0.83$, $A = 0.928$, $C = 0.026$, $\alpha = 1.232$. Other conditions as in fig. 3.

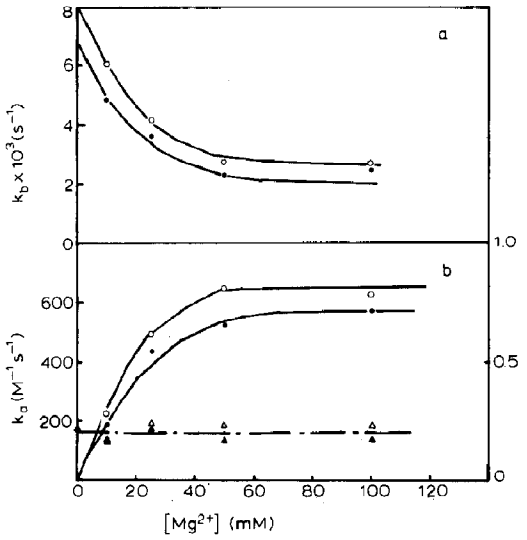

Fig. 6. (a) Dependence of dissociation rate constant k_b [(●) from R_g, (○) from $I(0)$] on Mg^{2+} concentration. (b) Dependence of association rate constant k_a [(●) from R_g, (○) from $I(0)$; scale on the right and tetramer fraction at time $t = 0$, W_0 [(▲) from R_g, (△) from $I(0)$; scale on the left] on Mg^{2+} concentration. k_a, k_b and W_0 were obtained by fitting the experimental time course to eq. 12 or 13 with $\alpha = 1.232$ and various W_{eq} values listed in table 1.

4.2. Stopped-flow X-ray scattering

Two solutions (A and B) were mixed and the scattered X-rays from the combined solutions were monitored. Solution A contains phosphorylase *b*, the other containing 2 mM AMP and various concentrations of magnesium acetate. Fig. 3 depicts the X-ray scattering patterns at different times. Both R_g and $I(0)$ were estimated for each time interval and plotted vs. time (figs. 4 and 5). However, no association kinetics were observed in terms of R_g and $I(0)$ in the absence of Mg^{2+} irrespective of the AMP concentration; $I(0)$ in the presence of AMP is greater than that in its absence by a factor of 1.22 (data not shown).

Fig. 6 shows the dependence of the rate constants and the tetramer fraction at $t = 0$ on Mg^{2+} concentration. In the presence of 1 mM AMP and 10 mM Mg^{2+}, the results are in agreement with those obtained from light scattering [21].

5. Discussion

(i) The recent availability of the stopped-flow X-ray scattering method represents a powerful tool for performing kinetic studies on conformational changes in biological macromolecules. In particular, the zero-angle scattering intensity in every case undergoes changes with alterations in molecular weight upon progression of the reaction. This makes it possible for one to elucidate the relation between association or dissociation processes in oligomeric enzymes and their biological function.

(ii) The burst phases in both R_g and $I(0)$ were detected during the initial stage of the reaction (< 0.5 s) in the presence of both AMP and Mg^{2+}. Since the amplitude of the burst phase appears to be independent of Mg^{2+} concentration, it is probable that very rapid association of the AMP-enzyme complex takes place prior to the 'slow' association upon formation of the ternary complex with AMP and Mg^{2+} which has been monitored by stopped-flow X-ray scattering. A possible explanation is that, if Mg^{2+} binding to the enzyme-AMP complex is diffusion-controlled, therefore reaching equilibrium rapidly enough, the burst phase seems to imply that conformational change of phosphorylase *b* occurs after Mg^{2+} binding to the enzyme-AMP complex. Either the conformational change itself proceeds slowly or a relatively slow association occurs after the conformational change of the enzyme.

When the rapid equilibrium condition mentioned above is satisfied, individual Mg^{2+} binding to the dimeric and tetrameric forms with different numbers of bound Mg^{2+} remains in equilibrium during tetramerization. The association process between a dimer with i Mg^{2+} and another with j Mg^{2+} is then expressed as:

$$D(Mg^{2+})_i + D(Mg^{2+})_j \rightleftharpoons T(Mg^{2+})_{i+j}.$$

According to the Adair equation, the concentration of dimer with i Mg^{2+} is

$$\frac{[D^*] A_i [Mg^{2+}]^i}{\sum_i A_i [Mg^{2+}]^i} \qquad (14)$$

where A_i designates the Adair constant. Similarly, the concentration of tetramer which is a complex of the dimer with i Mg^{2+} and the other with j Mg^{2+} can be written with Adair constant B_{ij} as:

$$\frac{[T^*]B_{ij}[Mg^{2+}]^{i+j}}{\sum_i \sum_j B_{ij}[Mg^{2+}]^{i+j}}. \tag{15}$$

Similarly to the manner proposed by Wang and Tsou [22], the rate constants for this reaction can be described:

$$k_a = \frac{\sum_i \sum_j k_{ij} A_i A_j [Mg^{2+}]^{i+j}}{\left(\sum_i A_i [Mg^{2+}]^i\right)^2} \tag{16}$$

$$k_b = \frac{\sum_i \sum_j k_{-ij} B_{ij} [Mg^{2+}]^{i+j}}{\sum_i \sum_j B_{ij} [Mg^{2+}]^{i+j}} \tag{17}$$

It is obvious that both k_a and k_b are functions of Mg^{2+} concentration as shown in fig. 6. In principle, we could determine the constants in eqs. 16 and 17 by curve fitting. However, in practice, the number of parameters in these equations is too large for one to be able to extract realistic parameters. However, it may be possible to simulate the trends of the rate constants with respect to Mg^{2+} concentration in a qualitative manner.

(iii) Using the average value of α in table 1 (1.232), the radius of gyration of the AMP-ligated tetramer R_T is calculated to be $39.32 \times 1.232 = 48.4 \pm 0.6$ Å, in good agreement with that of phosphorylase *a* in the absence of ligand [23], but at variance with the value of 50.2 ± 0.75 Å estimated by Puchwein et al. [20]. In the present study, no correction was made for slit smearing. We conclude that this apparent inconsistency in the R_g value for the tetramer is not due to slit smearing as described in item iv, but probably arises from the difference in equations used for estimation of the apparent R_g (cf. eq. 4 with eq. 8 in ref. 20).

The scattering intensity of the binary system is expressed as a linear combination of those of the dimer and tetramer:

$$I(h) = 0.5WI_T(h) + (1 - W)I_D(h). \tag{18}$$

Individual scattering intensities are described as:

$$I(h) = F^2(0)\left[1 - (1/3)R_g^2h^2 + \cdots\right]$$

$$I_T(h) = F_T^2(0)\left[1 - (1/3)R_T^2h^2 + \cdots\right]$$

$$I_D(h) = F_D^2(0)\left[1 - (1/3)R_D^2h^2 + \cdots\right]$$

where F represents the structure factor for each species. Therefore, we obtain the following relations.

$$F^2(0) = 0.5WF_T^2(0) + (1 - W)F_D^2(0)$$

$$F^2(0)R_g^2 = 0.5WF_T^2(0)R_T^2 + (1 - W)F_D^2(0)R_D^2$$

$$R_g^2 = \frac{0.5WF_T^2(0)R_T^2 + (1 - W)F_D^2(0)R_D^2}{0.5WF_T^2(0) + (1 - W)F_D^2(0)}$$

$$= \frac{0.5WN_T^2R_T^2 + (1 - W)N_D^2R_D^2}{0.5WN_T^2 + (1 - W)N_D^2} \tag{19}$$

where N_T and N_D denote the number of electrons contained in the tetramer and dimer, respectively. Assuming that the number of electrons of the tetramer and dimer are proportional to their molecular weights, eq. 19 can be written in the form of eq. 4. Hence, eq. 8 in ref. 20 may be incorrect.

(iv) In the present study, no correction was made for slit smearing. We calculated ideal and slit-smeared scattering curves for spheres of uniform density of radii 50 and 60 Å with the use of the optical parameters of our X-ray measurement system. Guinier plots of these data provided R_g and $I(0)$. Differences in R_g values calculated from the ideal and slit-smeared curves amounted to 0.025% for a 50 Å sphere and 0.039% for a 60 Å sphere. Differences in $I(0)$ were also estimated as 1.13% for a sphere of 50 Å and 0.85% for a sphere of 60 Å. In the current study, we estimated the tetramer fraction W at various Mg^{2+} concentrations by using the value of $I(0)/I_D(0)$. The difference in $I(0)_{60}/I(0)_{50}$ calculated for the ideal and smeared curves was estimated as 0.148%.

(v) Usually, the concentration of phosphorylase *b* in vivo is about 10^{-7} M. This value is much

lower than the dissociation constant of tetrameric phosphorylase *b* ($K_d = k_b/k_a = 10^{-5}$ M). Hence, phosphorylase *b* appears to be only in the dimeric form under physiological conditions. It is most likely that the dimer-tetramer interconversion of phosphorylase *b* may be independent of its catalytic function.

Acknowledgements

The authors are indebted to Dr. T. Furuno, Institute of Physical and Chemical Research, for fruitful discussions on scattering theory, and to Mr. K. Kimura, Dokkyo University School of Medicine, for support in computation.

References

1 D.J. Graves and J.H. Wang, in: The enzymes, vol. 7, 3rd edn., ed. P.D. Boyer (Academic Press, New York, 1972) p. 435.
2 H.J. Ho and J.H. Wang, Biochemistry 12 (1973) 4750.
3 M. Morange, F. Garcia Blanco, B. Vandenbunder and H. Buc, Eur. J. Biochem. 65 (1976) 553.
4 L.L. Kastenschmidt, J. Kastenschmidt and E. Helmreich, Biochemistry 7 (1968) 4543.
5 A. Guinier and G. Fournet, Small-angle scattering of X-rays (Wiley, New York, 1955).
6 M.H.J. Koch, H.B. Stuhrmann, P. Vachette and A. Tardieu, in: Uses of synchrotron radiation in biology, ed. H.B. Stuhrmann (Academic Press, London, 1983) p. 225.
7 G. Porod, in: Small angle X-ray scattering, eds. O. Glatter and O. Kratky (Academic Press, London, 1982) p. 17.
8 I. Pilz, O. Glatter and O. Kratky, Methods Enzymol. 61 (1979) 148.
9 M.F. Moody, P. Vachette, A.M. Foote, A. Tardieu, M.H.J. Koch and J. Bordas, Proc. Natl. Acad. Sci. U.S.A. 77 (1980) 4040.
10 A.G. Fowler, A.M. Foote, M.F. Moody, P. Vachette, S.W. Provencher, A. Gabriel, J. Bordas and M.H.J. Koch, J. Biophys. Biochem. Methods 7 (1983) 317.
11 Y. Inoko, H. Kihara and M.H.J. Koch, Biophys. Chem. 17 (1983) 171.
12 M. Cuillel, C. Berthet-Colominas, B. Krop, A. Tardieu, P. Vachette and B. Jacrot, J. Mol. Biol. 164 (1983) 645.
13 E.M. Fischer and E.G. Krebs, J. Biol. Chem. 231 (1957) 65.
14 M.H. Buc, U. Ullman, M. Goldberg and H. Buc, Biochimie 53 (1971) 283.
15 G.H. Fiske and Y. Subbarow, J. Biol. Chem. 66 (1925) 375.
16 L.F. Leloir and C.E. Cardini, Methods Enzymol. 3 (1957) 840.
17 T. Nagamura, K. Kurita, E. Tokikura and H. Kihara, J. Biochem. Biophys. Methods 11 (1985) 277.
18 Y. Amemiya, K. Wakabayashi, T. Hamanaka, T. Wakabayashi, T. Matsushita and H. Hashizume, Nuclear Instrum. Methods 208 (1983) 471.
19 T. Furuno, A. Ikegami, H. Kihara, M. Yoshida and Y. Kagawa, J. Mol. Biol. 170 (1983) 137.
20 G. Puchwein, O. Kratky, C.F. Golker and E. Helmreich, Biochemistry 9 (1970) 4691.
21 F. Munoz, M.A. Valles, J. Donoso, G. Echevarria and F.G. Blanco, J. Biochem. 94 (1983) 1649.
22 Z.-X. Wang and C.L. Tsou, J. Theor. Biol. 127 (1987) 253.
23 H. Kihara, T. Furuno, A. Ikegami and M.H.J. Koch, Biochem. (Life Sci. Adv.) 6 (1987) 211.